



Original article

Synthesis, antiproliferative activity and DNA binding study of mixed ammine/cyclohexylamine platinum(II) complexes with 1-(substituted benzyl) azetidine-3, 3-dicarboxylates

Yanyan Sun^{a,b}, Shaohua Gou^{a,b,*}, Runting Yin^{a,b}, Pingyuan Jiang^{a,b}

^a Pharmaceutical Research Center, School of Chemistry & Chemical Engineering, Southeast University, Nanjing 211189, China

^b Jiangsu Province Hi-Tech Laboratory for Bio-medical Research, Southeast University, Nanjing 211189, China

ARTICLE INFO

Article history:

Received 17 May 2011

Received in revised form

18 August 2011

Accepted 19 August 2011

Available online 26 August 2011

Keywords:

Platinum(II) complex

Cytotoxicity

Acute toxicity

Apoptosis

DNA cleavage

ABSTRACT

A novel series of ammine/cyclohexylamine platinum(II) complexes with 1-(substituted benzyl) azetidine-3, 3-dicarboxylates as leaving groups have been synthesized and characterized. All complexes were characterized by elemental analysis, IR, ¹H NMR, and ESI-MS spectra. The in vitro antiproliferative activities of the platinum-based compounds have been investigated against several human cancer cell lines, indicating that complexes **1** and **11** showed comparable cytotoxicity to those of cisplatin and oxaliplatin against four cell lines, superior to that of carboplatin. The results of drug safety evaluation (acute toxicity study) showed that complex **11** was much less toxic than cisplatin and oxaliplatin. Flow cytometry and agarose gel electrophoresis studies revealed that both complexes **1** and **11** induced apoptosis of tumor cells and demonstrated the binding affinity of complexes with pET22b plasmid DNA.

© 2011 Elsevier Masson SAS. All rights reserved.

1. Introduction

In clinical practice, platinum-based complexes have belonged to the most widely used antineoplastic drugs since the serendipitous discovery of the antitumor activity of cisplatin by Rosenberg and his co-workers in 1960's [1]. Cisplatin(cis-diamminedichloridoplatinum(II), Fig. 1) is one of the most active chemotherapeutic agents available for the treatment of a variety of malignant tumors such as testicular and ovarian cancers [2,3]. Despite its success, cisplatin has several shortcomings including toxicity (ototoxicity, neurotoxicity, gastrointestinal toxicity, renal and hepatic toxicity), low water-solubility, narrow spectrum of activity, and intrinsic or acquired resistance to limit its clinical application to the treatment of ovarian, head and neck, and testicular tumors [4,5]. In order to overcome these drawbacks, thousands of platinum complexes have been synthesized and evaluated as potential antitumor agents according to the structure-activity relationships (SAR) summarized by Cleare and Hoeschele in 1973 [6,7]. So far several platinum drugs have been screened and used in clinical practice including carboplatin and oxaliplatin (Fig. 1) as the typical delegates of the second and third generation of platinum-based antitumor agents,

respectively [8]. Furthermore, some research progress has been made in non-classical platinum-based complexes violating the classic structure-activity relationships, such as orally active platinum(IV) complexes, sterically hindered platinum(II) complexes, trans-platinum complexes, multinuclear platinum complexes, sulfur-containing platinum complexes [9–13], and so on.

Satraplatin [bis-acetato-ammine-dichlorido-cyclohexylamine platinum(IV), JM216, Fig. 1] as the first orally active platinum drug showed promise against second-line hormone refractory prostate cancer in phase III trials [14,15]. The two axial acetate groups of satraplatin which make the complex more lipophilic increase the oral bioavailability. After entering blood satraplatin is metabolized into bivalent platinum complex, named JM118 (cis-ammine dichloro (cyclohexylamine) platinum(II), Fig. 1), structurally similar to cisplatin by replacing one of the amine groups with a cyclohexylamine group [16]. JM118 which binds chemically to DNA by a similar mechanism to cisplatin is considerably more active than cisplatin against both cisplatin sensitive and resistant human tumor cells, although there are some differences in DNA binding mode between JM118 and cisplatin [17,18]. In view of the success of JM-216 in phase I and II clinical trials, many mixed ammine/amine platinum(II) complexes analogous to JM-118, the metabolite of JM-216, have been synthesized chemically and tested for anticancer activity against various human solid tumor cell lines

* Corresponding author. Tel./fax: +86 25 83272381.

E-mail address: sgou@seu.edu.cn (S. Gou).

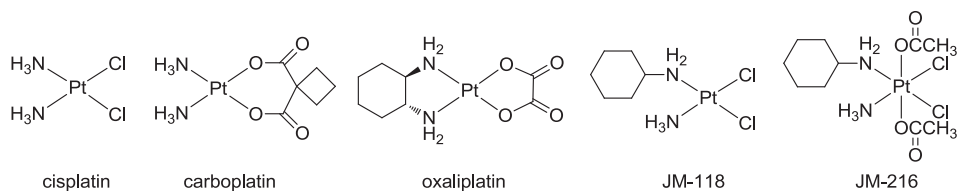


Fig. 1. Chemical structures of cisplatin, carboplatin, oxaliplatin, JM-118 and satraplatin.

by some researchers. Mixed ammine/cyclohexylamine platinum(II) complexes with carboxylates as leaving groups have demonstrated activity *in vitro* against EJ (human bladder carcinoma), HCT-8 (human colon carcinoma), BGC-823 (human gastric carcinoma), HL-60 (human immature granulocyte leukemia) and MCF-7 (human galactophore carcinoma) cell lines [19]. Besides, the platinum(II) complexes with ammine/cyclohexylamine as carrier ligands and dicarboxylates as leaving groups showed considerable cytotoxic activity against EJ and HL-60 cell lines and several complexes displayed cytotoxicity superior to that of cisplatin [20].

It is known to all that carboplatin shows decreased nephrotoxic and neurotoxic side effects compared with cisplatin because of the decreased reactivity of the dicarboxylate group. Besides, in view of the mixed ammine/amine platinum(II) complexes with chloro ions as leaving groups (for example, JM-118) showing low water-solubility, we chose a series of 1-(substituted benzyl) azetidine-3, 3-dicarboxylates as leaving groups to take the place of chloro ions and carboxylates in order to adjust the water-solubility, and used ammine/cyclohexylamine and cyclohexylamine/amine as carrier groups. In this study, a series of mixed ammine/amine platinum(II) complexes were synthesized and the antitumor activities against four human cancer cell lines were investigated. Besides, this paper summarizes the mechanism of the resulting compounds inducing cellular death and the influence of the compounds on the structure of DNA.

2. Results and discussion

2.1. Characterization

The synthesized platinum(II) complexes were characterized by elemental analysis, IR, ¹H NMR, and ESI-MS spectra. Infrared data of all complexes are showed in Table 1. The N–H stretching vibrations of complexes (1–11) show, in the range 3069–3209 cm⁻¹, red shifting compared with the single amino group, due to the amino group coordinating with Pt(II) ions. The ν_{as}(C–O) vibration of the complexes appears between 1603 and 1623 cm⁻¹ which is characteristic of coordinated carboxylate ligands [23], while the ν_s(C–O) vibration exhibits in 1380–1407 cm⁻¹. The values of Δν

Table 1
Infrared data^a (cm⁻¹) for the platinum(II) complexes.

Compd.	ν(N–H)	ν(C–H)	ν _{as} (C–O)	ν _s (C–O)	Δν	ν(Pt–O)	ν(Pt–N)
1	3208,3123	2931,2854	1616	1384	232	601	490
2	3195,3105	2932,2855	1616	1383	233	570	481
3	3196,3111	2932,2856	1614	1384	230	568	461
4	3200,3114	2932,2855	1604	1384	220	551	472
5	3187,3069	2932,2855	1610	1383	227	566	463
6	3209,3124	2933,2856	1623	1381	242	606	475
7	3184,3050	2934,2856	1617	1407	210	573	466
8	3192,3103	2932,2856	1616	1384	232	611	463
9	3197,3115	2932,2855	1622	1380	242	582	479
10	3205,3108	2930,2855	1615	1385	230	552	483
11	3202,3113	2931,2854	1603	1383	220	580	470
12	3199,3112	2931,2854	1604	1381	223	571	474
13	3194,3084	2933,2855	1609	1396	213	566	462

^a Selected infrared data are showed in this form; Δν = ν_{as}(C–O) – ν_s(C–O).

(ν_{as}(C–O) – ν_s(C–O)) of these complexes are in the range of 210–242 cm⁻¹, greater than 200 cm⁻¹, which supports the structure of the resulting complexes with bidentate coordination carboxylate ligands [24]. Besides, the fact that the carboxylate anion and the amino groups are coordinated to the metal atom is confirmed by the presence of ν (Pt–O) and ν (Pt–N) in 461–611 cm⁻¹. All the platinum complexes show 100% of [M + H]⁺ peaks in the ESI-MS spectra, which have three protonated ion peaks, respectively, because of the existence of the isotopes ¹⁹⁴Pt (33%), ¹⁹⁵Pt (34%), and ¹⁹⁶Pt (25%). ¹H NMR spectra are compatible to the chemical structures of the corresponding complexes.

2.2. In vitro cytotoxic activity

The antitumor activity of mixed ammine/amine platinum(II) complexes 1–11 and positive controls were assayed *in vitro* against HepG-2 (human hepatocellular carcinoma), MCF-7 (human breast carcinoma), A549 (human non-small cell lung cancer) and HCT-116 (human colorectal cancer) cell lines, respectively. The corresponding IC₅₀ values are listed in Table 2. It was noticed that the complexes (1, 5, 7, 9, 11 and 12) showed comparable cytotoxicity against four carcinoma cell lines to those of carboplatin and oxaliplatin, and the cytotoxicity of complex 6 against HepG-2 and MCF-7 cell lines was greater than the other carcinoma cell lines. Especially, complexes 1 and 11 had comparable cytotoxicity against HepG-2, MCF-7, and A549 to that of cisplatin. According to the comparison of IC₅₀ values of the complexes and positive controls toward four cell lines, the order of antitumor effect was 11 (R = 2-OCH₃) > 1 (R = H) > 12 (R = 3-OCH₃) > 9 (R = 3-CH₃) > 7 (R = 4-Cl) > 5 (R = 2-Cl) against four cell lines as a whole. It was observed in Table 2 that complex 11 was the most effective agent among the

Table 2
In vitro cytotoxicity (IC₅₀, μM)^a of all complexes against human tumor cell lines.

Compd.	R	IC ₅₀ (μM)			
		HepG-2 ^b	MCF-7 ^c	A549 ^d	HCT-116 ^e
1	H	7.92	9.81	8.11	6.04
2	<i>o</i> -F	>100	>100	>100	>100
3	<i>m</i> -F	>100	43.9	>100	34.9
4	<i>p</i> -F	>100	>100	>100	>100
5	<i>o</i> -Cl	31.1	24.3	30.5	25.0
6	<i>m</i> -Cl	27.9	14.7	54.1	51.3
7	<i>p</i> -Cl	20.7	18.6	24.3	17.2
8	<i>o</i> -CH ₃	>100	>100	>100	>100
9	<i>m</i> -CH ₃	24.2	10.9	24.6	10.2
10	<i>p</i> -CH ₃	76.3	>100	>100	52.1
11	<i>o</i> -OCH ₃	4.46	8.53	5.92	9.83
12	<i>m</i> -OCH ₃	9.27	13.5	25.2	13.0
13	<i>p</i> -OCH ₃	>100	>100	>100	>100
Cisplatin		1.96	5.53	5.33	n.d. ^f
Carboplatin		13.7	51.7	9.90	n.d.
Oxaliplatin		n.d.	n.d.	n.d.	3.32

^a IC₅₀ is the drug concentration effective in inhibiting 50% of the cell growth measured by the MTT assay after 72 h drug exposure.

^b Human hepatocellular carcinoma cell line.

^c Human breast carcinoma cell line.

^d Human non-small cell lung cancer cell line.

^e Human colorectal cancer cell line.

^f n.d. = not determined.

synthesized complexes, which was 1.1–2.2-fold less potent than cisplatin and 2.9-fold less potent than oxaliplatin in terms of IC_{50} , but 1.6–6.0-fold more potent than carboplatin. The second was complex **1**, approximately 5-fold more potent than carboplatin against MCF-7 cell line, while it showed cytotoxicity close to carboplatin against A549. Although complex **1** was 1.8-fold less potent than oxaliplatin against HCT-116 cell line, it was 1.7-fold more potent than carboplatin against HepG-2.

From the data in Table 2, the order of the cytotoxic activity of complexes owning different substituents on the aryl ring was $R = OCH_3 > H > CH_3 > Cl > F$. Considering that different structures of the leaving groups determined different leaving velocity, the complexes (**1** and **11**) showed higher cytotoxicity than the others probably because the aryl moiety of the leaving group without a substituent or with a substituent ($R = 2-OCH_3$) had a different influence on the leaving ability and made the leaving group more unstable and reactive.

2.3. Acute toxicity of complex **11**

The acute toxicity study (Table 3) showed that the LD_{50} value of complex **11** was 108.9 mg/kg, less than those of cisplatin ($LD_{50} = 12.0$ mg/kg) and oxaliplatin ($LD_{50} = 20.0$ mg/kg), indicating that complex **11** was much less toxic than cisplatin and oxaliplatin. According to the behavior observation and histological examination of the dead mice, the toxicities induced by the platinum compound included inactivity, loss of weight, renal and gastrointestinal toxicity which may cause death of mice.

2.4. Apoptosis assay for complexes **1** and **11**

With the purpose of detecting in which way the platinum complexes induced cellular death (necrosis or apoptosis), studies of flow cytometry were performed on **1**, **11**, cisplatin and oxaliplatin [25]. These compounds were incubated for 24 h at a concentration of 50 μ M and the results were shown in Figs. 2 and 3. Four areas in the diagrams stand for necrotic cells (Q1, positive for PI and negative for annexin/FITC, left square on the top), live cells (Q3, negative for annexin and PI, left square at the bottom), late apoptosis or necrosis cells (Q2, positive for annexin and PI, right square on the top) and apoptosis cells (Q4, negative for PI and positive for annexin, right square at the bottom), respectively.

In Figs. 2 and 4, as for HCT-116 cell line, complex **11** showed the highest population of apoptotic cells (42.2%) of the tested compounds, 5.5-fold higher than cisplatin and 1.2-fold higher than oxaliplatin. And complex **1** produced a comparable population of apoptotic cells (32.2%) to complex **11**, 1.1-fold lower than oxaliplatin and 4.2-fold higher than cisplatin. With respect to MCF-7 cell line in Figs. 3 and 4, the population of apoptotic cells induced by complex **1** (58.0%) was 9.6-fold higher than that of oxaliplatin and was close to that of cisplatin. Complex **11** produced a slightly lower population of apoptotic cells (40.6%) than complex **1** and cisplatin, but 6.8-fold higher than oxaliplatin at the same concentration. The results above demonstrated that the synthesized compounds, in general, induced apoptosis of HCT-116 and MCF-7 tumor cells.

Table 3
Evaluation of the acute toxicity for complex **11** and positive controls.

Compd.	LD_{50} (mg/kg)
11	108.9 (95% confidence limits = 96.4–121.9)
Cisplatin	12.0 ^a
Oxaliplatin	20.0 ^a

^a The reported values of LD_{50} of cisplatin and oxaliplatin were 13.0 mg/kg [26] and 19.8 mg/kg [27], respectively.

2.5. Interaction with pET22b plasmid DNA

The DNA cleavage ability of complexes **1** and **11** was generally monitored by agarose gel electrophoresis, and the pET22b plasmid DNA was used as the target. Agarose gel electrophoresis using pET22b plasmid DNA in the presence of the resulting complexes and cisplatin was carried out, and the result was shown in Fig. 5. In the electrophoretogram, the untreated pET22b plasmid DNA, which mainly consisted of covalently closed circular (form I, ccc) and a small amount of open circular (form II, oc) bands, was used as negative control. When pET22b plasmid DNA was incubated with cisplatin and tested compounds at 37 °C for 24 h, it was observed that the mobility of the plasmid decreased in different degrees.

For cisplatin, linear DNA (form III) of pET22b plasmid, whose electrophoretic mobility was between covalently closed circular and open circular forms, increased with the increasing concentration of the drug. At high concentration of the drug (160 μ M), the linear form accounted for a large proportion of pET22b plasmid DNA incubated with cisplatin. With regard to complex **1**, a different pattern had been found that the supercoil DNA was sufficiently unwound at the concentration range tested, giving rise to linear DNA mostly. It was noticed that complex **1** induced conformational changes from helix DNA to linear DNA at low concentration (<20 μ M). When compound **11** was incubated with pET22b plasmid DNA, the decrease in electrophoretic mobility of closed circular DNA with the increasing concentration of compound **11** was observed, resulting in unwinding sufficiently of supercoil DNA to become linear DNA at high concentration of the compound. In general, it could be deduced that the order of pET22b plasmid DNA binding affinity was compound **1** > **11** > cisplatin. The behavior of plasmid DNA for the electrophoretic mobility observed from the electrophoretogram indicated that tested compounds induced conformational changes in the DNA helix including cisplatin due to covalent binding of the compounds with nucleotides.

3. Conclusions

A series of mixed ammine/cyclohexylamine platinum(II) complexes were synthesized and characterized in this study. Different leaving groups have been used, whereas the mixed ammine/cyclohexylamine as carrier groups was not changed. The results of in vitro antiproliferative activity suggested that complex **1** ($R = H$) and complex **11** ($R = 2-OCH_3$) showed cytotoxicity against four cell lines comparable to those of cisplatin and oxaliplatin, superior to that of carboplatin. And we found that methoxyl substituent group of the aryl ring had a more positive effect on the in vitro cytotoxicity than methyl, fluoro, and chloro substituents. According to the data of acute toxicity study, complex **11** exhibited much lower toxicity than cisplatin and oxaliplatin. Moreover, flow cytometry analysis concluded apoptosis mechanism of the resulting compounds inducing death of tumor cells by which cisplatin and oxaliplatin took effect. The interaction between the platinum complexes and pET22b plasmid DNA was investigated by agarose gel electrophoresis, indicating that selected compounds (**1** and **11**) displayed higher cleavage capability for pET22b plasmid DNA than cisplatin. In conclusion, it is worth studying complexes **1** and **11** further as antitumor agents for the treatment of human solid cancers.

4. Experimental

4.1. Chemistry

4.1.1. Materials and measurements

All reagents and chemicals were of analytical reagent grade and used without further purification. Potassium tetrachloroplatinate(II)

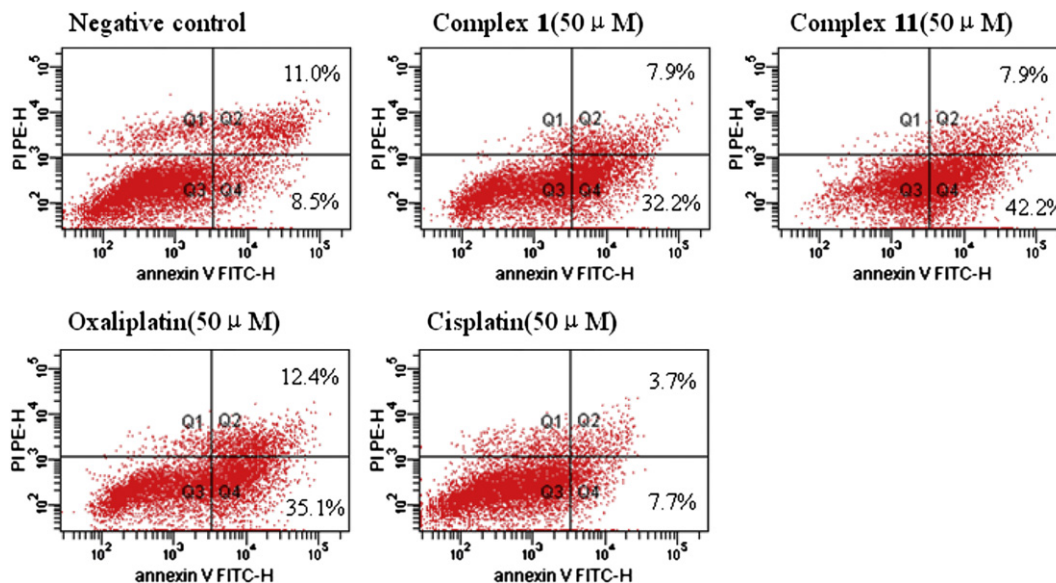


Fig. 2. Flow cytometric analysis of the distribution of HCT-116 cells treated with the selected compounds, oxaliplatin and cisplatin.

was purchased from a local chemical company. Elemental analyses for C, H and N were done on a Vario MICRO CHNOS Elemental Analyzer, Elementar. Infrared spectra were recorded in the range 400–4000 cm^{-1} and measured in KBr pellets on a Nicolet IR200 FT-IR spectrometer. The ^1H NMR spectra were recorded on a Bruker 500 MHz spectrometer. Mass spectra were measured on a Bruker Esquire ESI-MS instrument.

4.1.2. Synthesis of sodium 1-(substituted benzyl) azetidine-3, 3-dicarboxylate (L-1–L-13)

Compounds L-1–L-13 were synthesized according to the procedure as follows (Scheme 1).

Synthesis of L-1 (sodium 1-benzylazetidine-3, 3-dicarboxylate): 2.0 g of KHCO_3 (0.02 mol) and 15.4 g of formaldehyde (37% aqueous solution) were mixed, and stirred at 25–30 °C until the solution

turned to be a colorless and transparent liquid. To the mixture was added 16.0 g of diethyl malonate (0.1 mol). After stirring for 3 h at room temperature, 17.0 g of $(\text{NH}_4)_2\text{SO}_4$ in 50 ml water was added slowly to the resulting white turbid solution. The aqueous phase was extracted twice with ethyl (30 ml \times 2). The combined organic extracts were dried over anhydrous Na_2SO_4 and the solvent was evaporated in vacuo. 50 ml of isopropyl ether was added to the residue and the mixture was kept cool at –17 °C overnight, giving colorless crystals as the intermediate, diethyl 2,2-bis(hydroxymethyl)malonate.

To 100 ml of anhydrous acetonitrile was added 22.0 g of diethyl 2,2-bis(hydroxymethyl)malonate (0.1 mol) obtained in the first step. The resulting solution was stirred until the dissolution was complete. Then the solution was cooled to –20 °C, 59.5 g of trifluoromethanesulfonic anhydride (0.21 mol) was added dropwise with stirring for 40 min. To the mixture was added 65.0 g of

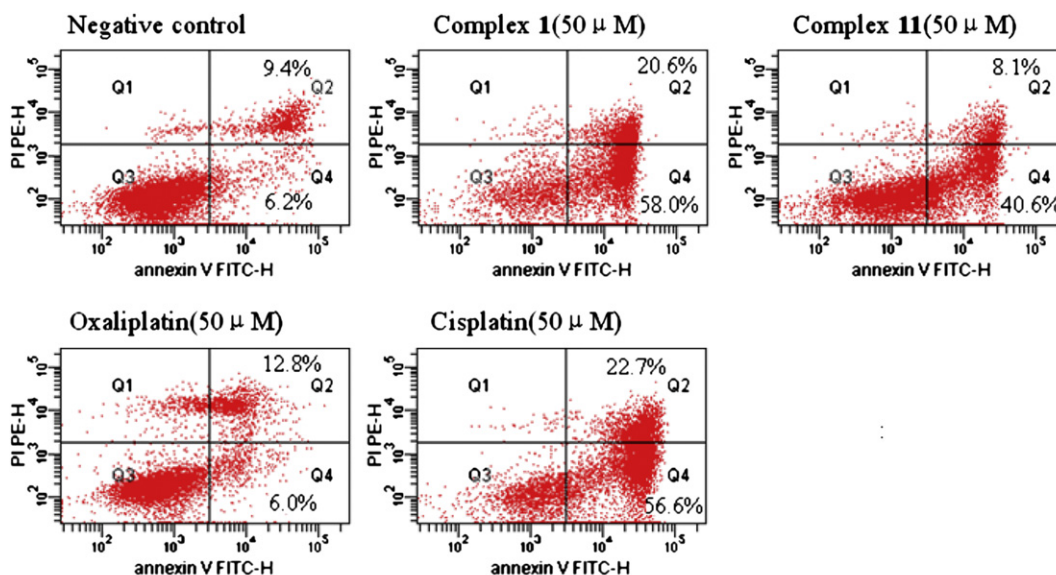


Fig. 3. Flow cytometric analysis of the distribution of MCF-7 cells treated with the selected compounds, oxaliplatin and cisplatin.

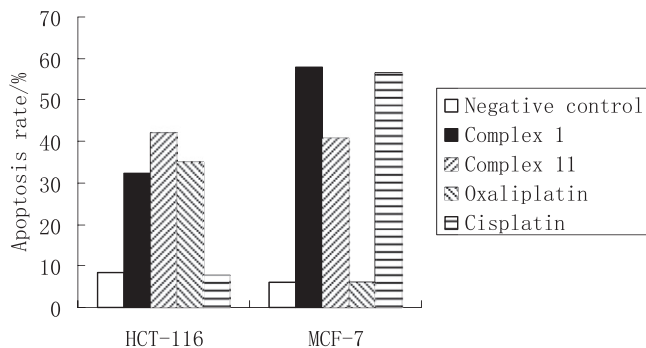


Fig. 4. The apoptosis rates of HCT-116 and MCF-7 cell lines induced by complexes **1** and **11** with cisplatin and oxaliplatin as controls. (HCT-116: colorectal cancer; MCF-7: breast carcinoma).

N-ethyl-diisopropylamine (0.5 mol) drop by drop at $-10\text{ }^{\circ}\text{C}$ for 1 h, followed by adding 12.8 g of benzylamine (0.12 mol). The mixture was stirred and refluxed for 2 h, and then cooled to the room temperature. 150 ml of toluene was added and the organic phase was washed twice with 150 ml of water. The solvent was evaporated in vacuo and the residue was added to 50 ml of methanol. 30 ml of sodium hydroxide solution (10 mol/l) was carefully added to the stirred mixture at room temperature and the mixture was kept stirring for 2 h at $50\text{ }^{\circ}\text{C}$. After cooling to the room temperature, the resulting white solids were filtered off and washed twice with methanol. The white product was dried at $30\text{ }^{\circ}\text{C}$ in vacuo.

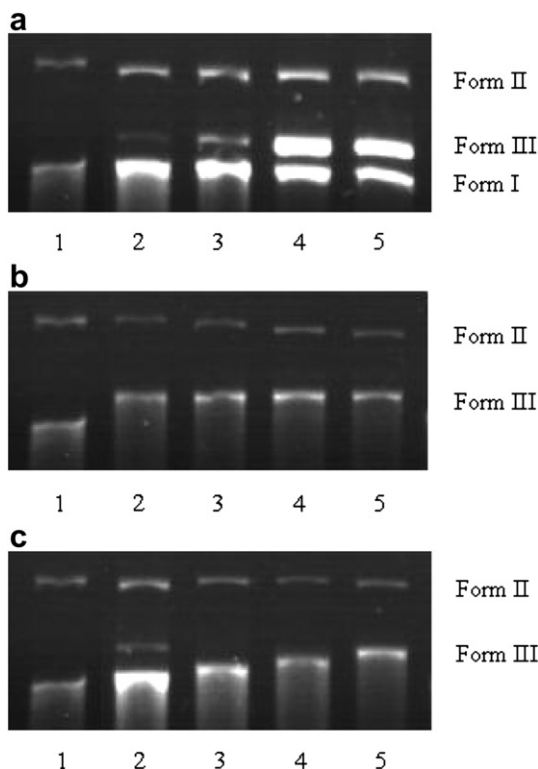


Fig. 5. Gel electrophoretic mobility pattern of pET22b plasmid DNA incubated with various concentrations of platinum compounds, (a) cisplatin, (b) compound **1**, (c) compound **11**. The lanes (from left to right) correspond to untreated plasmid DNA only (lane 1), then concentrations of 20, 40, 80, and $160\text{ }\mu\text{M}$ of cisplatin, and tested compounds incubated with DNA (lanes 2–5).

The preparation of L-2–L-13 was the same as that of L-1 described above by replacing benzylamine with substituted benzylamine.

L-1: Yield 81%. White powder. Anal. calcd. for $\text{C}_{12}\text{H}_{11}\text{NO}_4\text{Na}_2$: C, 51.62; H, 3.97; N, 5.02. Found: C, 51.52; H, 3.99; N, 5.10. IR (KBr, cm^{-1}): 3420(br), 2956, 2845, 1611, 1474, 1433, 1333, 745, 694; ^1H NMR (d_6 - $\text{D}_2\text{O}/\text{TMS}$, ppm): δ 3.40(s, 4H, CH_2 of azetidine), δ 3.48(s, 2H, NCH_2Ph), δ 7.12–7.21(m, 5H, CH of Ph); ESI-MS: m/z $[\text{M} - 2\text{Na} + \text{H}]^- = 234(100\%)$.

L-2: Yield 78%. White powder. Anal. calcd. for $\text{C}_{12}\text{H}_{10}\text{FNO}_4\text{Na}_2$: C, 48.50; H, 3.39; N, 4.71. Found: C, 48.48; H, 3.35; N, 4.83. IR (KBr, cm^{-1}): 3436(br), 2849, 1612, 1437, 1334, 760; ^1H NMR (d_6 - $\text{D}_2\text{O}/\text{TMS}$, ppm): δ 3.64(s, 4H, CH_2 of azetidine), δ 3.73(s, 2H, NCH_2Ph), δ 7.11–7.36(m, 4H, CH of Ph); ESI-MS: m/z $[\text{M} - 2\text{Na} + \text{H}]^- = 252(100\%)$.

L-3: Yield 76%. White powder. Anal. calcd. for $\text{C}_{12}\text{H}_{10}\text{FNO}_4\text{Na}_2$: C, 48.50; H, 3.39; N, 4.71. Found: C, 48.55; H, 3.36; N, 4.80. IR (KBr, cm^{-1}): 3428(br), 2844, 1613, 1438, 1335, 878, 794, 683; ^1H NMR (d_6 - $\text{D}_2\text{O}/\text{TMS}$, ppm): δ 3.60(s, 4H, CH_2 of azetidine), δ 3.78(s, 2H, NCH_2Ph), δ 7.04–7.41(m, 4H, CH of Ph); ESI-MS: m/z $[\text{M} - 2\text{Na} + \text{H}]^- = 252(100\%)$.

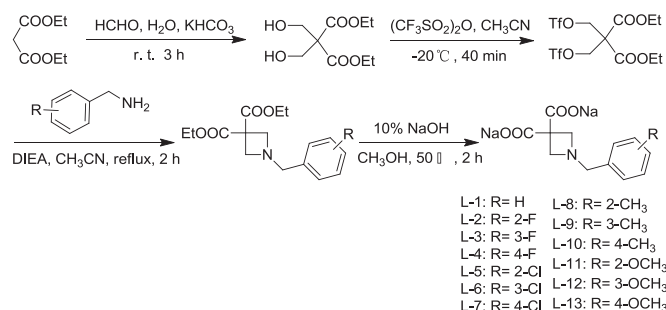
L-4: Yield 74%. White powder. Anal. calcd. for $\text{C}_{12}\text{H}_{10}\text{FNO}_4\text{Na}_2$: C, 48.50; H, 3.39; N, 4.71. Found: C, 48.47; H, 3.49; N, 4.64. IR (KBr, cm^{-1}): 3410(br), 2850, 1610, 1437, 1334, 835; ^1H NMR (d_6 - $\text{D}_2\text{O}/\text{TMS}$, ppm): δ 3.58(s, 4H, CH_2 of azetidine), δ 3.65(s, 2H, NCH_2Ph), δ 7.08–7.34(m, 4H, CH of Ph); ESI-MS: m/z $[\text{M} - 2\text{Na} + \text{H}]^- = 252(100\%)$.

L-5: Yield 83%. White powder. Anal. calcd. for $\text{C}_{12}\text{H}_{10}\text{ClNO}_4\text{Na}_2$: C, 45.95; H, 3.21; N, 4.47. Found: C, 45.79; H, 3.31; N, 4.53. IR (KBr, cm^{-1}): 3421(br), 2850, 1609, 1434, 1334, 763; ^1H NMR (d_6 - $\text{D}_2\text{O}/\text{TMS}$, ppm): δ 3.57(s, 4H, CH_2 of azetidine), δ 3.71(s, 2H, NCH_2Ph), δ 7.15–7.33(m, 4H, CH of Ph); ESI-MS: m/z $[\text{M} - 2\text{Na} + \text{H}]^- = 268(100\%)$.

L-6: Yield 81%. White powder. Anal. calcd. for $\text{C}_{12}\text{H}_{10}\text{ClNO}_4\text{Na}_2$: C, 45.95; H, 3.21; N, 4.47. Found: C, 45.87; H, 3.28; N, 4.51. IR (KBr, cm^{-1}): 3400(br), 2849, 1608, 1437, 1334, 871, 771, 695; ^1H NMR (d_6 - $\text{D}_2\text{O}/\text{TMS}$, ppm): δ 3.49(s, 4H, CH_2 of azetidine), δ 3.55(s, 2H, NCH_2Ph), δ 7.11–7.22(m, 4H, CH of Ph); ESI-MS: m/z $[\text{M} - 2\text{Na} + \text{H}]^- = 268(100\%)$.

L-7: Yield 82%. White powder. Anal. calcd. for $\text{C}_{12}\text{H}_{10}\text{ClNO}_4\text{Na}_2$: C, 45.95; H, 3.21; N, 4.47. Found: C, 45.98; H, 3.25; N, 4.51. IR (KBr, cm^{-1}): 3424(br), 2846, 1611, 1436, 1334, 799; ^1H NMR (d_6 - $\text{D}_2\text{O}/\text{TMS}$, ppm): δ 3.55(s, 4H, CH_2 of azetidine), δ 3.61(s, 2H, NCH_2Ph), δ 7.16–7.28(m, 4H, CH of Ph); ESI-MS: m/z $[\text{M} - 2\text{Na} + \text{H}]^- = 268(100\%)$.

L-8: Yield 90%. White powder. Anal. calcd. for $\text{C}_{13}\text{H}_{13}\text{NO}_4\text{Na}_2$: C, 53.25; H, 4.47; N, 4.78. Found: C, 53.16; H, 4.59; N, 4.62. IR (KBr, cm^{-1}): 3430(br), 2850, 1606, 1436, 1333, 767; ^1H NMR (d_6 - $\text{D}_2\text{O}/$



Scheme 1. Synthesis of the ligands (L-1–L-13).

TMS, ppm): δ 2.29(s, 3H, CH_3Ph), δ 3.68(s, 4H, CH_2 of azetidine), δ 3.73(s, 2H, NCH_2Ph), δ 7.26–7.27(m, 4H, CH of Ph); ESI-MS: m/z $[M - 2Na + H]^- = 248$ (100%).

L-9: Yield 81%. White powder. Anal. calcd. for $C_{13}H_{13}NO_4Na_2$: C, 53.25; H, 4.47; N, 4.78. Found: C, 53.33; H, 4.62; N, 4.58. IR (KBr, cm^{-1}): 3420(br), 2853, 1607, 1433, 1334, 857, 781, 690; 1H NMR (d_6 - D_2O /TMS, ppm): δ 2.34(s, 3H, CH_3Ph), δ 3.59(s, 4H, CH_2 of azetidine), δ 3.63(s, 2H, NCH_2Ph), δ 7.14–7.30(m, 4H, CH of Ph); ESI-MS: m/z $[M - 2Na + H]^- = 248$ (100%).

L-10: Yield 83%. White powder. Anal. calcd. for $C_{13}H_{13}NO_4Na_2$: C, 53.25; H, 4.47; N, 4.78. Found: C, 53.29; H, 4.52; N, 4.70. IR (KBr, cm^{-1}): 3426(br), 2848, 1609, 1435, 1333, 805; 1H NMR (d_6 - D_2O /TMS, ppm): δ 2.16(s, 3H, CH_3Ph), δ 3.56(s, 4H, CH_2 of azetidine), δ 3.61(s, 2H, NCH_2Ph), δ 7.09 (m, 4H, CH of Ph); ESI-MS: m/z $[M - 2Na + H]^- = 248$ (100%).

L-11: Yield 79%. White powder. Anal. calcd. for $C_{13}H_{13}NO_5Na_2$: C, 50.49; H, 4.24; N, 4.53. Found: C, 50.54; H, 4.29; N, 4.48. IR (KBr, cm^{-1}): 3425(br), 2855, 1611, 1433, 1333, 770; 1H NMR (d_6 - D_2O /TMS, ppm): δ 3.55(s, 4H, CH_2 of azetidine), δ 3.62(s, 2H, NCH_2Ph), δ 3.75(s, 3H, $PhOCH_3$), δ 7.11(s, 4H, CH of Ph); ESI-MS: m/z $[M - 2Na + H]^- = 264$ (100%).

L-12: Yield 85%. White powder. Anal. calcd. for $C_{13}H_{13}NO_5Na_2$: C, 50.49; H, 4.24; N, 4.53. Found: C, 50.60; H, 4.32; N, 4.45. IR (KBr, cm^{-1}): 3420(br), 2830, 1604, 1434, 1334, 850, 771, 689; 1H NMR (d_6 - D_2O /TMS, ppm): δ 3.59(s, 4H, CH_2 of azetidine), δ 3.65(s, 2H, NCH_2Ph), δ 3.82(s, 3H, $PhOCH_3$), δ 6.91–7.34(m, 4H, CH of Ph); ESI-MS: m/z $[M - 2Na + H]^- = 264$ (100%).

L-13: Yield 76%. White powder. Anal. calcd. for $C_{13}H_{13}NO_5Na_2$: C, 50.49; H, 4.24; N, 4.53. Found: C, 50.39; H, 4.34; N, 4.46. IR (KBr, cm^{-1}): 3426(br), 2843, 1609, 1433, 1334, 803; 1H NMR (d_6 - D_2O /TMS, ppm): δ 3.50(s, 4H, CH_2 of azetidine), δ 3.54(s, 2H, NCH_2Ph), δ 3.69(s, 3H, $PhOCH_3$), δ 6.85–7.17(m, 4H, CH of Ph); ESI-MS: m/z $[M - 2Na + H]^- = 264$ (100%).

4.1.3. Synthesis of complexes 1–13

The preparation of target complexes 1–13 was carried out as shown in Scheme 2. The brown yellow intermediate cis - $[Pt(C_6H_{11}NH_2)(NH_3)_2]$ was synthesized according to the literature [21]. The corresponding silver 1-(substituted benzyl) azetidine-3, 3-dicarboxylate was prepared by the reaction of sodium 1-(substituted benzyl) azetidine-3, 3-dicarboxylate related and silver nitrate in water.

Synthesis of complex 1: The intermediate cis - $[Pt(C_6H_{11}NH_2)(NH_3)_2]$ (2 mmol) was suspended in 100 ml of distilled water, and then the freshly prepared silver 1-benzylazetidine-3, 3-dicarboxylate (2 mmol) was added. The reaction mixture was heated to 50 °C and stirred for 24 h in dark under a nitrogen atmosphere. Then the mixture was cooled to the room temperature, and AgI deposits were filtered off and washed with water. The yellow filtrate was concentrated by a rotary evaporator and then kept cool at 4 °C for several hours. The resulting yellow crystals

were filtered off, washed with a little of chilled water, and then dried at 40 °C in vacuo.

The preparation of compounds 2–13 was the similar to that of compound 1 described above.

Complex 1: Yield 55%. Yellow crystals. Anal. calcd. for $C_{18}H_{27}N_3O_4Pt$: C, 39.70; H, 5.00; N, 7.72. Found: C, 39.62; H, 5.09; N, 7.85. IR (KBr, cm^{-1}): 3420(br), 3208, 3123, 2931, 2854, 1616, 1451, 1384, 747, 699; 1H NMR (d_6 - D_2O /TMS, ppm): δ 0.81–2.61(m, 11H, CH_2 and CH of cyclohexyl), δ 3.90–4.32(m, 6H, CH_2N), δ 7.37–7.45(m, 5H, CH of Ph); ESI-MS: m/z $[M + H]^+ = 545$ (100%).

Complex 2: Yield 60%. Yellow crystals. Anal. calcd. for $C_{18}H_{26}FN_3O_4Pt$: C, 38.43; H, 4.66; N, 7.47; Found: C, 38.50; H, 4.62; N, 7.39. IR (KBr, cm^{-1}): 3404(br), 3195, 3105, 2932, 2855, 1616, 1453, 1383, 762; 1H NMR (d_6 - D_2O /TMS, ppm): δ 0.82–2.27(m, 11H, CH_2 and CH of cyclohexyl), δ 3.80–4.23(m, 6H, CH_2N), δ 7.17–7.22(m, 4H, CH of Ph); ESI-MS: m/z $[M + H]^+ = 563$ (100%).

Complex 3: Yield 51%. Yellow crystals. Anal. calcd. for $C_{18}H_{26}FN_3O_4Pt$: C, 38.43; H, 4.66; N, 7.47; Found: C, 38.52; H, 4.71; N, 7.43. IR (KBr, cm^{-1}): 3410 (br), 3196, 3106, 2932, 2856, 1614, 1449, 1384, 788, 686; 1H NMR (d_6 - D_2O /TMS, ppm): δ 1.08–2.27(m, 11H, CH_2 and CH of cyclohexyl), δ 3.80–4.52(m, 6H, CH_2N), δ 7.15–7.30(m, 4H, CH of Ph); ESI-MS: m/z $[M + H]^+ = 563$ (100%).

Complex 4: Yield 58%. Yellow crystals. Anal. calcd. for $C_{18}H_{26}FN_3O_4Pt$: C, 38.43; H, 4.66; N, 7.47; Found: C, 38.34; H, 4.56; N, 7.45. IR (KBr, cm^{-1}): 3408(br), 3200, 3114, 2932, 2855, 1604, 1449, 1384, 829, 769; 1H NMR (d_6 - D_2O /TMS, ppm): δ 0.95–2.29(m, 11H, CH_2 and CH of cyclohexyl), δ 3.77–4.33(m, 6H, CH_2N), δ 7.19–7.23(m, 4H, CH of Ph); ESI-MS: m/z $[M + H]^+ = 563$ (100%).

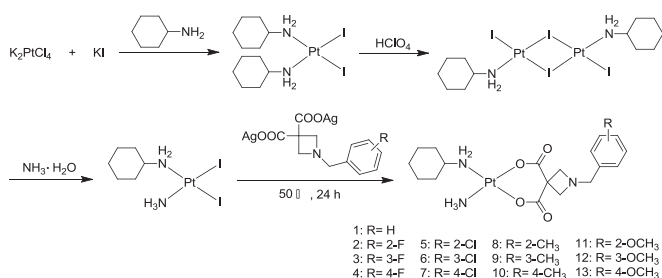
Complex 5: Yield 49%. Yellow crystals. Anal. calcd. for $C_{18}H_{26}ClN_3O_4Pt$: C, 37.34; H, 4.53; N, 7.26. Found: C, 37.37; H, 4.39; N, 7.38. IR (KBr, cm^{-1}): 3406(br), 3187, 3069, 2932, 2855, 1610, 1442, 1390, 757; 1H NMR (d_6 - D_2O /TMS, ppm): δ 1.12–2.29(m, 11H, CH_2 and CH of cyclohexyl), δ 3.78–4.30(m, 6H, CH_2N), δ 7.17–7.22(m, 4H, CH of Ph); ESI-MS: m/z $[M + H]^+ = 580$ (100%).

Complex 6: Yield 59%. Yellow crystals. Anal. calcd. for $C_{18}H_{26}ClN_3O_4Pt$: C, 37.34; H, 4.53; N, 7.26. Found: C, 37.40; H, 4.42; N, 7.31. IR (KBr, cm^{-1}): 3420(br), 3209, 3124, 2933, 2856, 1623, 1449, 1381, 784, 682; 1H NMR (d_6 - D_2O /TMS, ppm): δ 1.26–2.19(m, 11H, CH_2 and CH of cyclohexyl), δ 3.77–4.34(m, 6H, CH_2N), δ 7.30–7.38(m, 4H, CH of Ph); ESI-MS: m/z $[M + H]^+ = 580$ (100%).

Complex 7: Yield 55%. Yellow crystals. Anal. calcd. for $C_{18}H_{26}ClN_3O_4Pt$: C, 37.34; H, 4.53; N, 7.26. Found: C, 37.43; H, 4.45; N, 7.34. IR (KBr, cm^{-1}): 3385(br), 3184, 3050, 2934, 2856, 1617, 1407, 1348, 844, 802; 1H NMR (d_6 - D_2O /TMS, ppm): δ 1.08–2.19(m, 11H, CH_2 and CH of cyclohexyl), δ 3.78–4.32(m, 6H, CH_2N), δ 7.20–7.25(m, 4H, CH of Ph); ESI-MS: m/z $[M + H]^+ = 580$ (100%).

Complex 8: Yield 62%. Yellow crystals. Anal. calcd. for $C_{19}H_{29}N_3O_4Pt$: C, 40.86; H, 5.23; N, 7.52. Found: C, 40.77; H, 5.18; N, 7.66. IR (KBr, cm^{-1}): 3398(br), 3192, 3103, 2932, 2856, 1616, 1450, 1383, 749; 1H NMR (d_6 - D_2O /TMS, ppm): δ 1.10–2.30(m, 11H, CH_2 and CH of cyclohexyl), δ 2.36(s, 3H, CH_3Ph), δ 4.05–4.52(m, 6H, CH_2N), δ 7.16–7.32(m, 4H, CH of Ph); ESI-MS: m/z $[M + H]^+ = 559$ (100%).

Complex 9: Yield 57%. Yellow crystals. Anal. calcd. for $C_{19}H_{29}N_3O_4Pt$: C, 40.86; H, 5.23; N, 7.52. Found: C, 40.75; H, 5.15; N, 7.62. IR (KBr, cm^{-1}): 3399(br), 3197, 3115, 2932, 2855, 1622, 1449, 1380, 784, 683; 1H NMR (d_6 - D_2O /TMS, ppm):



Scheme 2. Synthesis of the complexes (1–13).

δ 1.09–2.34(m, 11H, CH_2 and CH of cyclohexyl), δ 2.38(s, 3H, CH_3Ph), δ 3.95–4.32(m, 6H, CH_2N), δ 7.10–7.35(m, 4H, CH of Ph); ESI-MS: m/z $[M + H]^+ = 559(100\%)$.

Complex **10**: Yield 58%. Yellow crystals. Anal. calcd. for $C_{19}H_{29}N_3O_4Pt$: C, 40.86; H, 5.23; N, 7.52. Found: C, 40.80; H, 5.26; N, 7.57. IR (KBr, cm^{-1}): 3411(br), 3205, 3114, 2930, 2855, 1615, 1449, 1383, 815, 770; 1H NMR (d_6 - D_2O/TMS , ppm): δ 1.14–2.33(m, 11H, CH_2 and CH of cyclohexyl), δ 2.39(s, 3H, CH_3Ph), δ 4.00–4.55(m, 6H, CH_2N), δ 7.26–7.39(m, 4H, CH of Ph); ESI-MS: m/z $[M + H]^+ = 559(100\%)$.

Complex **11**: Yield 54%. Yellow crystals. Anal. calcd. for $C_{19}H_{29}N_3O_5Pt$: C, 39.72; H, 5.09; N, 7.31. Found: C, 39.70; H, 5.18; N, 7.29. IR (KBr, cm^{-1}): 3385(br), 3202, 3113, 2931, 2854, 1603, 1451, 1383, 754; 1H NMR (d_6 - D_2O/TMS , ppm): δ 1.19–2.30(m, 11H, CH_2 and CH of cyclohexyl), δ 3.91–4.34(m, 6H, CH_2N), δ 4.41(s, 3H, $PhOCH_3$), δ 7.09–7.53(m, 4H, CH of Ph); ESI-MS: m/z $[M + H]^+ = 575(100\%)$.

Complex **12**: Yield 60%. Yellow crystals. Anal. calcd. for $C_{19}H_{29}N_3O_5Pt$: C, 39.72; H, 5.09; N, 7.31. Found: C, 39.59; H, 5.05; N, 7.42. IR (KBr, cm^{-1}): 3373(br), 3199, 3112, 2931, 2854, 1604, 1452, 1381, 786, 693; 1H NMR (d_6 - D_2O/TMS , ppm): δ 1.27–2.29(m, 11H, CH_2 and CH of cyclohexyl), δ 3.68–4.11(m, 6H, CH_2N), δ 4.35(s, 3H, $PhOCH_3$), δ 7.03–7.42(m, 4H, CH of Ph); ESI-MS: m/z $[M + H]^+ = 575(100\%)$.

Complex **13**: Yield 46%. Yellow crystals. Anal. calcd. for $C_{19}H_{29}N_3O_5Pt$: C, 39.72; H, 5.09; N, 7.31. Found: C, 39.65; H, 5.12; N, 7.34. IR (KBr, cm^{-1}): 3394(br), 3194, 3084, 2933, 2855, 1609, 1447, 1396, 854, 825; 1H NMR (d_6 - D_2O/TMS , ppm): δ 1.18–2.34(m, 11H, CH_2 and CH of cyclohexyl), δ 3.79–4.16(m, 6H, CH_2N), δ 4.29(s, 3H, $PhOCH_3$), δ 7.07–7.44(m, 4H, CH of Ph); ESI-MS: m/z $[M + H]^+ = 575(100\%)$.

4.2. Biological studies

4.2.1. Cell culture

The *in vitro* antitumor activities of all platinum complexes were tested against four kinds of human solid tumor cell lines including HepG-2 (human hepatocellular carcinoma), MCF-7 (human breast carcinoma), A549 (human non-small cell lung cancer) and HCT-116 (human colorectal cancer). The cell lines were cultured in RPMI-1640 medium supplemented with 10% fetal bovine serum (FBS), 100 μ g/ml of penicillin and 100 μ g/ml of streptomycin in an atmosphere of 5% CO_2 at 37 °C.

4.2.2. Cytotoxicity analysis (IC_{50})

The IC_{50} (concentration of tested agent causing 50% inhibition of cell growth) values of all complexes were determined using the MTT assay [22]. This assay is based on the cleavage of the yellow tetrazolium salt (3-(4, 5-dimethylthiazol-2-yl)-2, 5-diphenyl tetrazolium bromide; MTT, Sigma) forming purple formazan crystals by viable cells. The cells were plated in 96-well culture plates at a density of 10^3 cells per well and incubated for 24 h at 37 °C in a 5% CO_2 incubator. The complexes were dissolved in H_2O and diluted to the required concentration (1, 2, 10, 20, 40, and 100 μ M) with culture medium. Then the diluted complexes were added to the wells, and the cells were incubated at 37 °C in a 5% CO_2 incubator for 72 h. After that, the cells were treated with 20 μ l MTT dye solution (5 mg/ml) for 4 h cultivation. The media with MTT solution were removed with DMSO solution (100 μ l). The absorbance was measured at 540 nm. The IC_{50} value was determined from the chart of cell viability (%) against dose of complex added (μ M).

4.2.3. Determination of acute toxicity (LD_{50})

LD_{50} values (median lethal dose) were determined with ICR mice of both sexes, weighting 18–22 g, for compound **11**. These

mice were divided into 4 groups, administered at the dose of 10, 30, 60, 90 and 120 mg/kg. The behavior of tested mice was observed for 7 days after tail intravenous injection. The LD_{50} values were calculated by Bliss method.

4.2.4. Flow cytometry analysis

The apoptosis induced by platinum complexes was determined by flow cytometry using an Annexin V-FITC Apoptosis Detection Kit (Roche, USA) according to the manufacturer's instructions. After induced apoptosis of selected cell lines (HCT-116 and MCF-7) by the addition of 50 μ M selected compounds and positive controls including cisplatin (50 μ M) and oxaliplatin (50 μ M) for 24 h, cells were collected by centrifugation for 5 min. Then cells were washed twice with cold water and resuspended in Annexin V-FITC binding buffer at a concentration of 1×10^6 cells/ml. Cells were stained with 5 μ l Annexin V-FITC and incubated in the dark at 25 °C for 10 min. Then the cell suspension was centrifugated for 5 min and cells were resuspended in Annexin V-FITC binding buffer. Propidium iodide (10 μ l) was added and the tubes were placed on ice and away from light. The fluorescence was measured using a flow cytometer (FAC Scan, Becton Dickenson, USA). The results were analyzed by using FCSEXPRESS software and represented as percentage of normal and apoptotic cells at various stages.

4.2.5. Gel electrophoresis study

Interaction of the platinum(II) complexes (compound **1** and **11**) with DNA was studied by agarose gel electrophoresis. Cisplatin was used as positive control, and pET22b plasmid DNA of 50 ng/ μ l concentration was used for the experiments. Appropriate dilutions of tested compounds were made, and the required volumes of solutions were added to the tubes to achieve a set of concentrations in the range of 0–160 μ M pET22b DNA (0.25 μ g, 5 μ l) was added to each tube. 2 μ l of charge maker was added to aliquot parts of 10 μ l of the drug-DNA mixtures. The platinum complexes were incubated with pET22b plasmid DNA at 37 °C for 24 h. After that, the agarose gel (ultra pure grade, Bio-Rad, made up to 1% w/v) containing ethidium bromide (1 μ g/ml) was prepared using 1 \times TA buffer (45 mM Tris-acetate, pH 7.5). The mixtures underwent electrophoresis in agarose gel in 1 \times TA buffer (45 mM Tris-acetate, pH 7.5) at 90 V for 1 h. The DNA bands were visualized with a Molecular Imager (Bio-Rad, USA).

Acknowledgments

This work is supported by the National Natural Science Foundation of China (Project 20971022) and the Six Top Talents Funding of Jiangsu Province (Project 2008046) as well as the New Drug Creation Project of the National Science and Technology Major Foundation of China (Project 2010ZX09401-401) to S.H. Gou. Sun would like to thank the Scientific Research Innovation Project for College Graduates of Jiangsu Province (Project CX10B_084Z) and Scientific Research Foundation of Graduate School of Southeast University (Project YBJJ1106).

References

- [1] B. Rosenberg, L. Van Camp, J.E. Trosko, V.H. Mansour, Nature 222 (1969) 385.
- [2] B. Lippert (Ed.), Cisplatin: Chemistry and Biochemistry of a Leading Anticancer Drug, Verlag Helvetica Chimica Acta, Zurich, Switzerland, 2000, p. 563.
- [3] M.A. Jakupec, M. Galanski, V.B. Arion, C.G. Hartinger, B.K. Keppler, Dalton Trans. (2008) 183–194.
- [4] M.A. Fuertes, C. Alonso, J.M. Perez, Chem. Rev. 103 (2003) 645–662.
- [5] S.W. Johnson, J.P. Stevenson, P.J. O'Dwyer, in: V.T. DeVita Jr., S. Hellman, S.A. Rosenberg (Eds.), Cisplatin and Its Analogues. In Cancer: Principles and Practice of Oncology, sixth ed. J. B. Lippincott Company, Philadelphia, PA, 2001, pp. 376–388.
- [6] M.J. Cleare, J.D. Hoeschele, Platinum Met. Rev. 17 (1973) 3–7.

- [7] M.J. Cleare, J.D. Hoeschele, *Bioinorg. Chem.* 2 (1973) 187–192.
- [8] E. Raymond, S. Faivre, S.G. Chaney, J.M. Woynarowski, E. Cvitkovic, *Mol. Cancer Ther.* 1 (2002) 227–235.
- [9] E. Wong, C.M. Giandomenico, *Chem. Rev.* 99 (1999) 2451–2466.
- [10] C.F. O'Neill, B. Koberle, J.R.W. Masters, L.R. Kelland, *Br. J. Cancer* 81 (1999) 1294–1303.
- [11] U. Bierbach, M. Sabat, N. Farrell, *Inorg. Chem.* 39 (2000) 1882–1890.
- [12] B.A.J. Jansen, J. Van Zwan, H. Dulk, J. Brouwer, J. Reedijk, *J. Med. Chem.* 44 (2001) 245–249.
- [13] L.H. Wang, Y. Liu, Q.D. You, S.H. Gou, *Prog. Chem.* 16 (2004) 456–461.
- [14] H. Kostrhunova, J. Kasparkova, D. Gibson, V. Brabec, *Mol. Pharm.* 7 (2010) 2093–2102.
- [15] P. Gramatica, E. Papa, M. Luini, *J. Biol. Inorg. Chem.* 15 (2010) 1157–1169.
- [16] H. Choy, C. Park, M. Yao, *Clin. Cancer Res.* 14 (2008) 1633–1638.
- [17] H. Kostrhunova, O. Vrana, T. Suchankova, D. Gibson, J. Kasparkova, V. Brabec, *Chem. Res. Toxicol.* 23 (2010) 1833–1842.
- [18] J.F. Hartwig, S.J. Lippard, *J. Am. Chem. Soc.* 114 (1992) 5646–5654.
- [19] J.C. Zhang, Y. Shen, M.S. Yang, *Chin. J. Inorg. Chem.* 22 (2006) 823–831.
- [20] J.C. Zhang, Y. Shen, *Synth. React. Inorg. Met.-Org. Chem.* 36 (2006) 345–351.
- [21] F.D. Rochon, P.C. Kong, *Can. J. Chem.* 64 (1986) 1894–1896.
- [22] T.R. Mosmann, *J. Immunol. Methods* 65 (1983) 55–63.
- [23] S. Al-Baker, R. Perez-Soler, A.R. Khokhar, *J. Coord. Chem.* 29 (1993) 1–6.
- [24] G.B. Deacon, R.J. Phillips, *Coord. Chem. Rev.* 33 (1980) 227–250.
- [25] A.M. Montana, F.J. Bernal, J. Lorenzo, C. Farnos, C. Batalla, M.J. Prieto, V. Moreno, F.X. Aviles, J.M. Mesas, M.T. Alegre, *Bioorg. Med. Chem.* 16 (2008) 1721–1737.
- [26] J. Zou, P.Y. Dou, K. Wang, *J. Inorg. Biochem.* 65 (1997) 145–149.
- [27] Y. Yu, L.G. Lou, W.P. Liu, H.J. Zhu, Q.S. Ye, X.Z. Chen, W.G. Gao, S.Q. Hou, *Eur. J. Med. Chem.* 43 (2008) 1438–1443.